Head and Neck Cancers

4

O. Rager, M. Becker, and A.J. Beer

Contents

Head and Neck Cancers

Head and neck cancers comprise about 5.5 % of all cancers worldwide. More than 90 % of head and neck malignancies are squamous cell carcinomas (HNSCC) mainly caused by tobacco and alcohol consumption. However, HNSCC caused by infection with the Human Papilloma Virus (HPV) type 16 and 18 are increasingly seen in younger adults, particularly in the oropharynx. These tumors are usually smaller and their prognosis is slightly better as compared to non HPV-related cancers.

Due to the rich lymphatic drainage, lymph node metastases are common and may even be seen in early tumors. The prevalence of lymph node metastases at initial presentation depends on the site of tumor origin and its presence affects overall survival considerably. A particular feature of HNSCC is the high rate of synchronous or metachronous second tumors, which are most often seen in the lung or esophagus.

Treatment of HNSCC includes surgery, radiation therapy ± chemotherapy or a combination of the two.

Because of its excellent soft tissue resolution, MRI is often used as a first line imaging modality for the assessment of loco-regional disease, whereas PET/CT is mainly used for the assessment of lymph node metastases, distant disease and for the detection of tumor recurrence after treatment. PET/MRI combines the advantages of both modalities and contributes to the diagnostic work up of these tumors.

O. Rager (✉)
Department of Imaging, Division of Nuclear Medicine and Molecular Imaging, Geneva University Hospital, Geneva, Switzerland
e-mail: olivier.rager@hcuge.ch

M. Becker
Department of Imaging, Division of Radiology, Geneva University Hospital, Geneva, Switzerland
e-mail: minerva.becker@hcuge.ch

A.J. Beer
Department of Nuclear Medicine, Klinikum Rechts der Isar, Technische Universität München, Munich, Germany

O. Ratib et al. (eds.), *Atlas of PET/MR Imaging in Oncology*,
DOI 10.1007/978-3-642-31292-2_4, © Springer-Verlag Berlin Heidelberg 2013

Squamous Cell Carcinoma of the Larynx

Clinical History

Fifty-three-year-old male. Consults for dysphonia and odynophagia since 5 months.

Tobacco: 120 pack years.

Alcohol: 50 g/day.

Because of increasing dyspnea, the patient underwent tracheotomy 10 days prior to imaging. A tumor lesion was seen endoscopically suggesting a squamous cell carcinoma. Prior to endoscopy, a [18F]FDG-PET/MRI was performed.

Imaging Technique

High-resolution [18F]FDG-PET/MRI with axial T2w SE and T1w SE images before and after injection of intravenous Gadolinium chelates (Gd). Axial high-resolution Dixon sequence after intravenous administration of Gd with sagittal and coronal 2D reformations. The axial MRI sequences were obtained using a 2–3 mm slice thickness, a field of view of 20 × 20 cm and a 512 × 512 matrix. MRI, PET and fused PET MRI images of the head and neck area are provided.

Findings

Hyperintense lesion on T2w images with heterogeneous enhancement after intravenous injection of Gadolinium chelates and with intense hypermetabolism on the PET acquisition. The transglottic mass infiltrates the thyroid cartilage and the pre-laryngeal soft tissues, the left cricoid and the left arythenoid cartilage. Moderate focal uptake around the tracheostomy. Large necrotic lymph node metastases are seen bilaterally in the neck involving levels III and V on the left side and levels II–IV on the right.

Teaching Points

Transglottic laryngeal HNSCC are aggressive tumors involving at least two of the laryngeal regions (supraglottic, glottic and subglottic). They typically invade the thyroid cartilage and may extend into the soft tissues in the neck (stage T4 according to UICC and AJCC guidelines). Tumor spread into the soft tissues in the neck may also occur not only through the cartilages but also through the thyrohyoid membrane.

Transglottic HNSCC often have lymph node metastases at initial presentation. Lymph node metastases are often necrotic. Necrosis is typically seen as hyperintense areas on T2w images and as non-enhancing areas after intravenous injection of Gd. FDG metabolism may be quite variable depending on the degree of necrosis.

Lymph node metastases typically involve several neck levels. If the subglottis is invaded, metastatic lymph nodes should be looked for in the upper mediastinum.

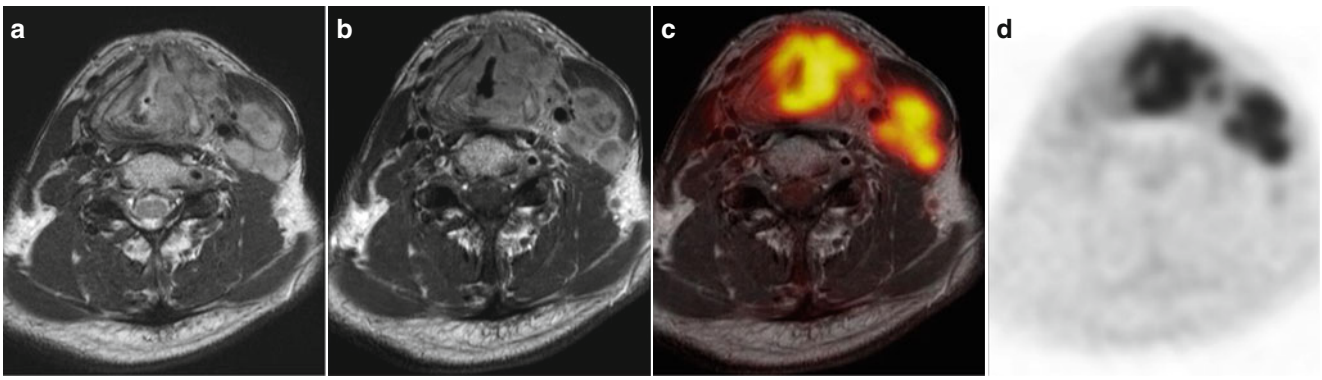

Fig. 4.1 Axial [18F]FDG-PET/MRI images at the level of the tumor: (**a**) T2w, (**b**) T1w + Gd, (**c**) fused T1w + PET, (**d**) PET. [18F]FDG-PET/MRI has the ability to precisely assess tumor spread as described above, in particular invasion of the laryngeal cartilages (thyroid, cricoid and arytenoid), extralaryngeal soft tissues, and submucosal spaces, as well the lymph node status, which is less well possible with PET/CT (Fig. 4.2)

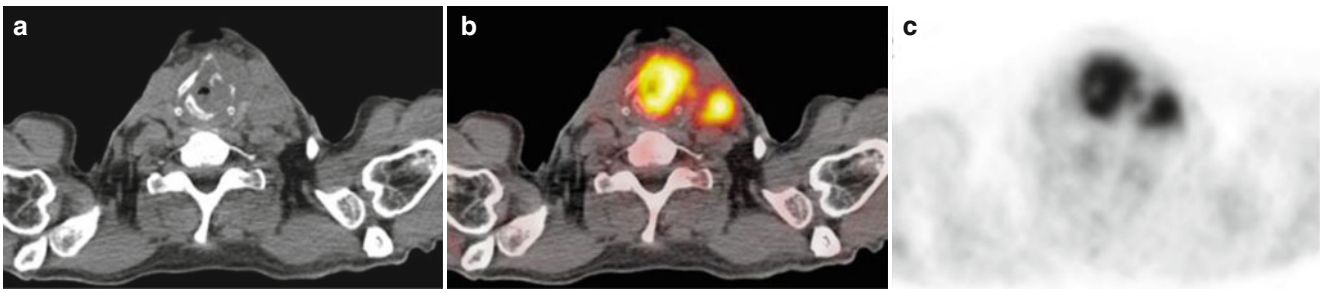

Fig. 4.2 Axial PET/CT obtained in the same patient shows the corresponding images at the level of the tumor: (**a**) CT (**b**) fused PET/CT (**c**) PET alone

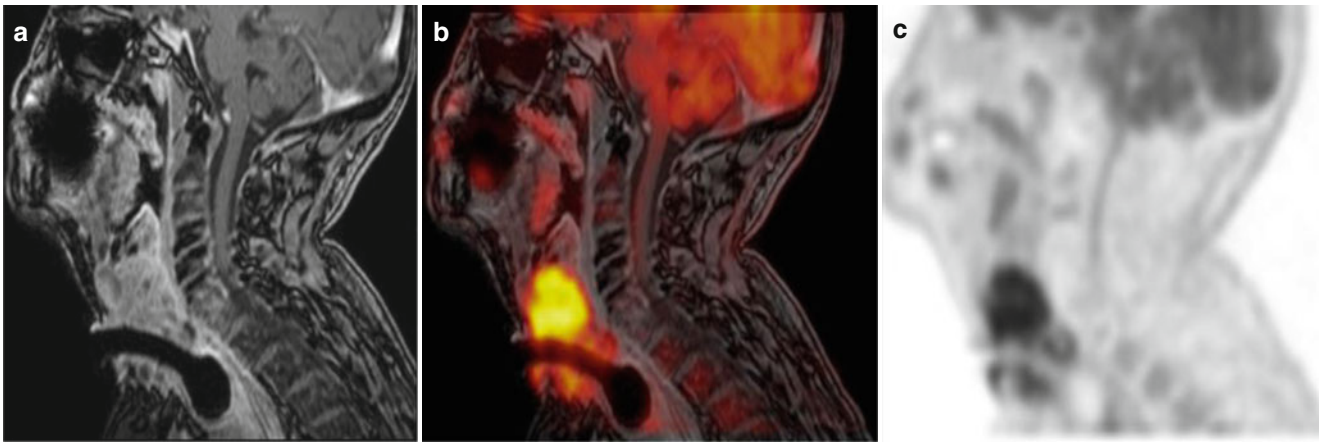

Fig. 4.3 Sagital PET/MR images: (**a**) sagittal 2D reformatted Dixon sequence, (**b**) fused sagittal Dixon images and PET image, (**c**) PET. The transglottic tumor spread is easily seen on these images. Note high metabolic uptake within the tumor and moderate hypermetabolism around tracheostomy corresponding to inflammatory changes

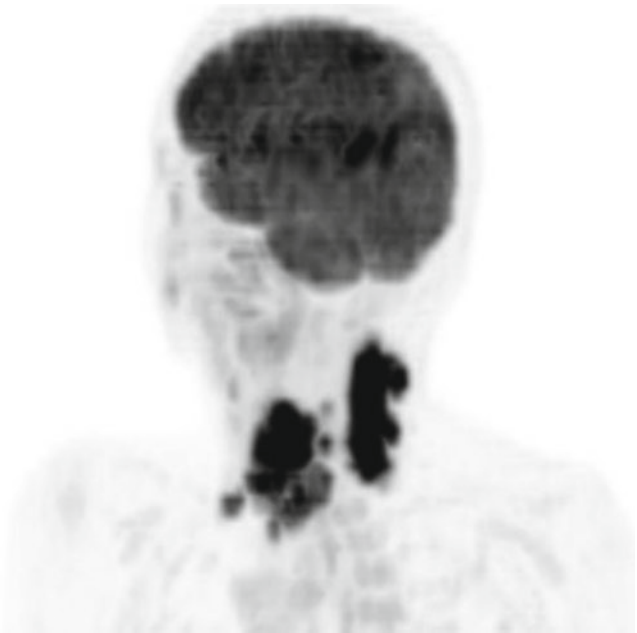

Fig. 4.4 Lateral oblique MIP PET scan showing the laryngeal tumor and bilateral involvement of lymph nodes

Oropharyngeal HNSCC

Clinical History

Fifty-seven years old male referred for restaging of a tonsillar tumor after radiotherapy and chemotherapy.

Smoker since 40 years, 1 package per day. The patient had endarterectomy of the left carotid and is currently treated for hypertension. Tongue pain since 3 months.

Imaging Technique

High-resolution [18F]FDG-PET/MRI with axial T2w SE and T1w SE images before and after injection of intravenous Gadolinium-chelates (Gd). The axial MRI sequences were obtained using a 2–3 mm slice thickness, a field of view of 20×20 cm and a 512×512 matrix. MRI, PET and fused [18F]FDG-PET/MRI images of the head and neck area and chest are provided.

Findings

Ulceration of the left amygdaloglossal sulcus with an area of necrosis seen on T2w images. No enhancing lesion is present after injection of Gd. Based on the MRI findings, the diagnosis is scar tissue. However, the hypermetabolic focus on the PET and on the fused [18F]FDG-PET/MRI images indicates the persistence of tumor. There is also a hypermetabolic lymph node in the left level II and a necrotic lymph node metastasis without hypermetabolism adjacent to it. Note the presence of a second lesion in the lung, which proved to be a synchronous lung tumor. The findings were confirmed surgically. However, the tumor size of the recurrent HNSCC was largely underestimated at [18F]FDG-PET/MRI.

Teaching Points

[18F]FDG-PET/MRI can identify distant metastases and synchronous tumors.

Although it can differentiate scar tissue and necrotic tissue from viable tumor, the size of the detected tumor may be grossly underestimated, as was the case here.

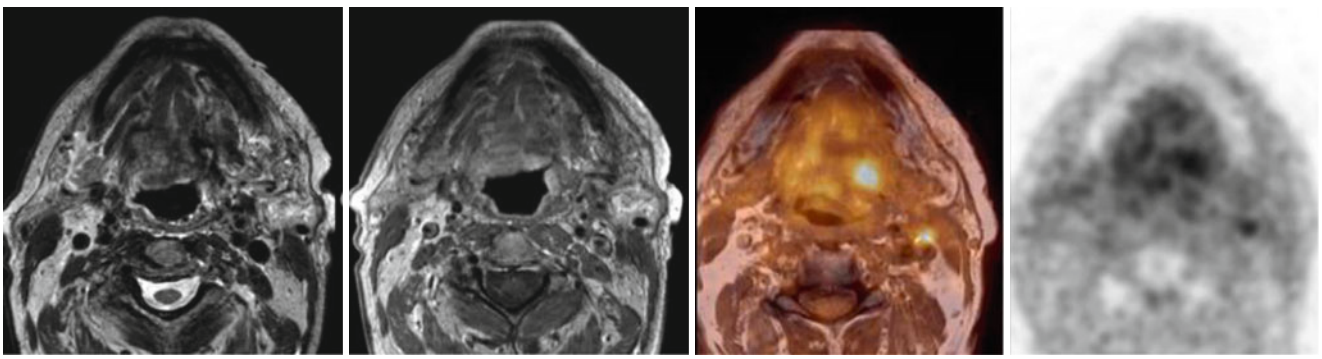

Fig. 4.5 Ulceration of the left amygdaloglossal sulcus with an area of necrosis surrounded by a low signal rim corresponding to scar tissue on T2w MR images. The focal FDG uptake suggested residual tumor

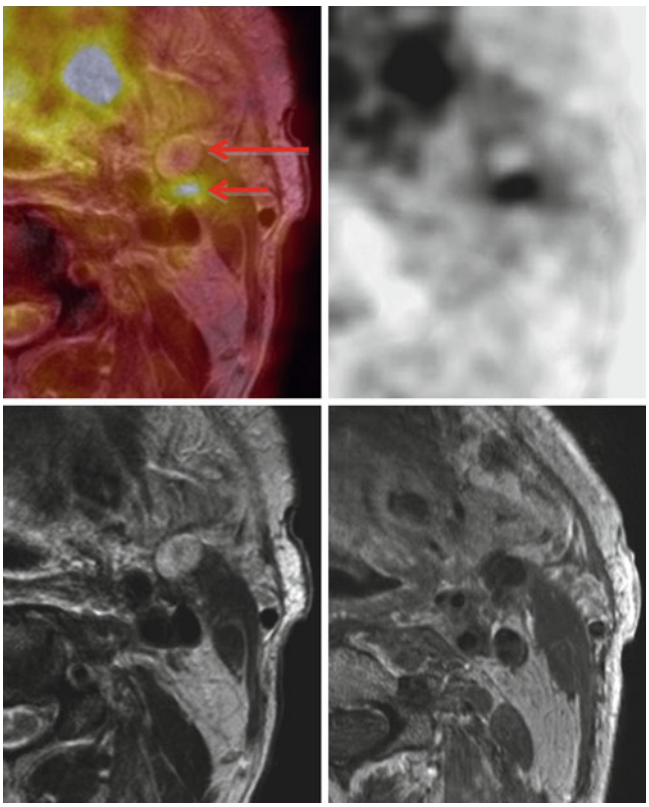

Fig. 4.6 A millimetric lymph node with intense hypermetabolism (shown with a *short red arrow*) and a necrotic lymph node metastasis with a peripheral halo of low metabolism (shown with *long red arrow*). Both lymph nodes were metastatic

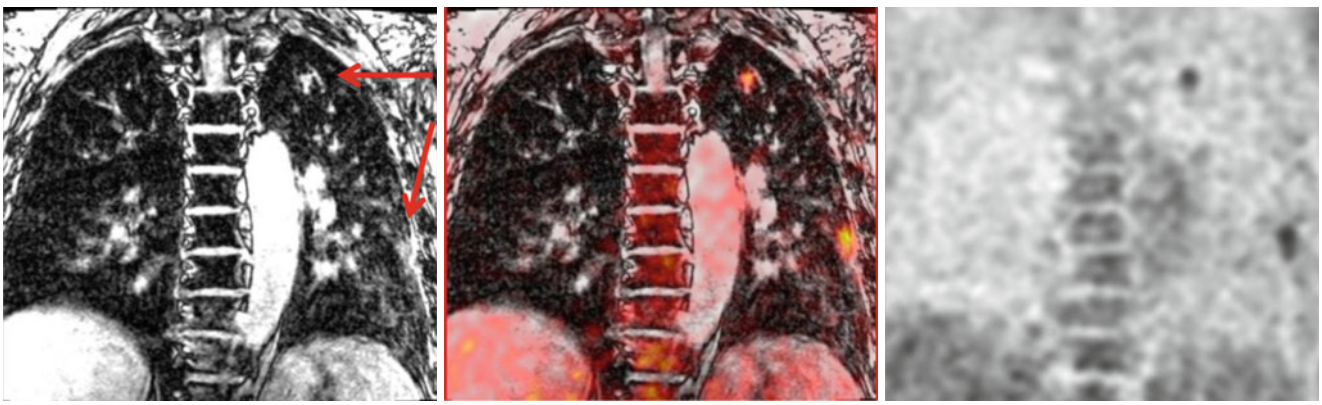

Fig. 4.7 Hypermetabolic lung nodule in the upper left lobe corresponding to a synchronous lung tumor versus a pulmonary metastasis. Biopsy revealed a second primary lung tumor. The focal uptake area in the apical segment of the inferior lobe corresponded to infectious disease

Lymphoma of the Nasal Fossa

Clinical History

Sixty-seven-year-old male in good general health with recent onset of asthenia, stuffy nose and sinusitis slowly progressing over several months. Antibiotic treatment did not improve symptoms. Clinical workup reveals a nasal mass and biopsy reveals a diffuse large B-cell lymphoma.

PET/MRI was performed for pre-treatment staging.

Imaging Technique

PET: 376 MBq 18F-FDG, 70 kg/174 cm patient, 240 min uptake time, 9 beds × 3 min.

MRI: T1w SE, 3DTFE (Act. TR/TE 6.2/3.0, $0.80 \times 1.03 \times 1.02$ mm^3).

Findings

Large hypermetabolic tumor mass of the left nasal cavity displacing and infiltrating the nasal septum and causing obstruction of the osteomeatal complex. Note mucous retention in the left maxillary sinus due to blocked drainage.

Teaching Points

Extranodal lymphomas are rare but may affect all head and neck localizations.

Lymphomatopus masses share common imaging characteristics due to their increased cellularity: low signal on T2-w sequences, low ADC values and high SUVmax values.

Despite their large size, major areas of necrosis are often absent resulting most often in characteristic homogenous enhancement patterns after intravenous administration of Gd.

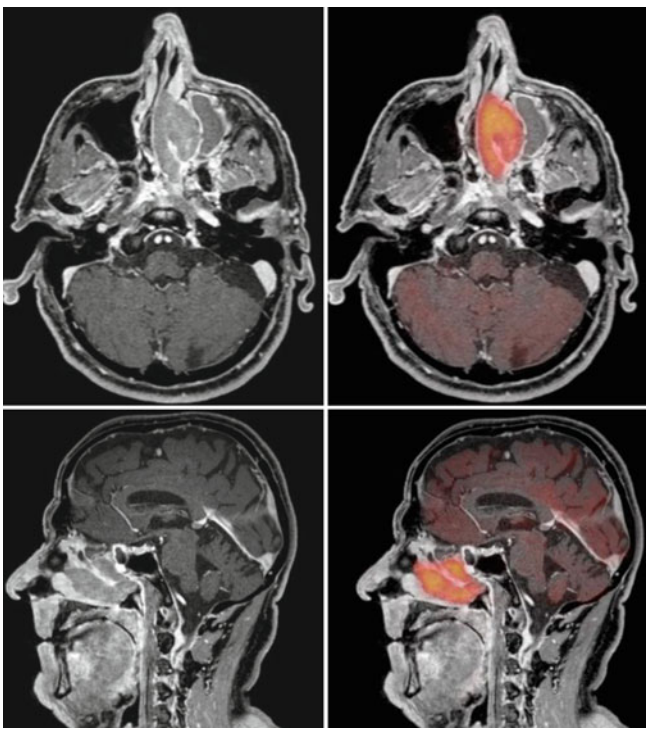

Fig. 4.8 Axial and sagittal 3D T1 TFE MRI images (*left*) and fused PET/MRI images (*right*) showing a large hypermetabolic mass in the left nasal fossa and ethmoid cells infiltrating the nasal septum and causing mucous retention in the left maxillary sinus

Fig. 4.9 Lateral oblique MIP image of the whole body PET scan showing the hypermetabolic lesion in the nasal fossa but no other distant lesions

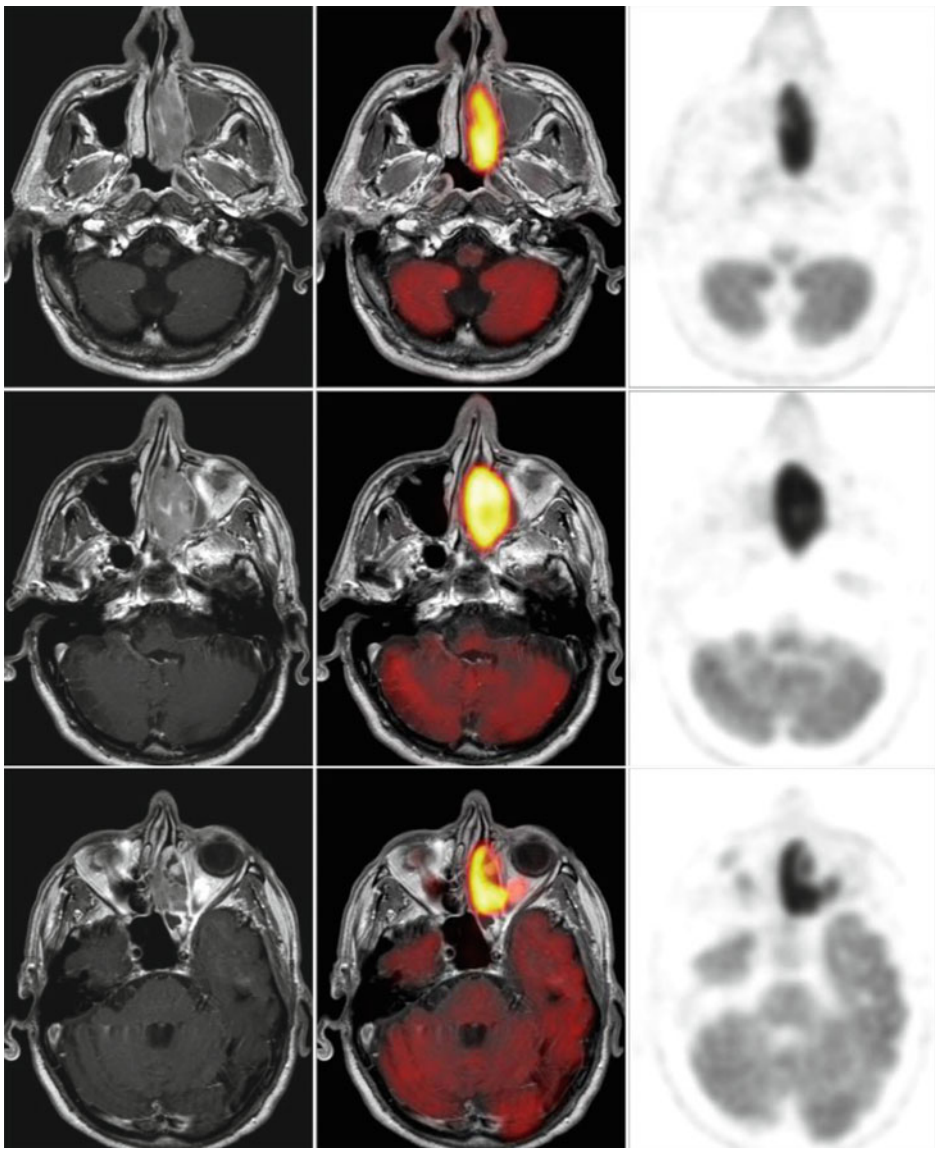

Fig. 4.10 Axial views obtained at three different levels with MRI (*left*) PET (*right*) and fused (*middle*) images

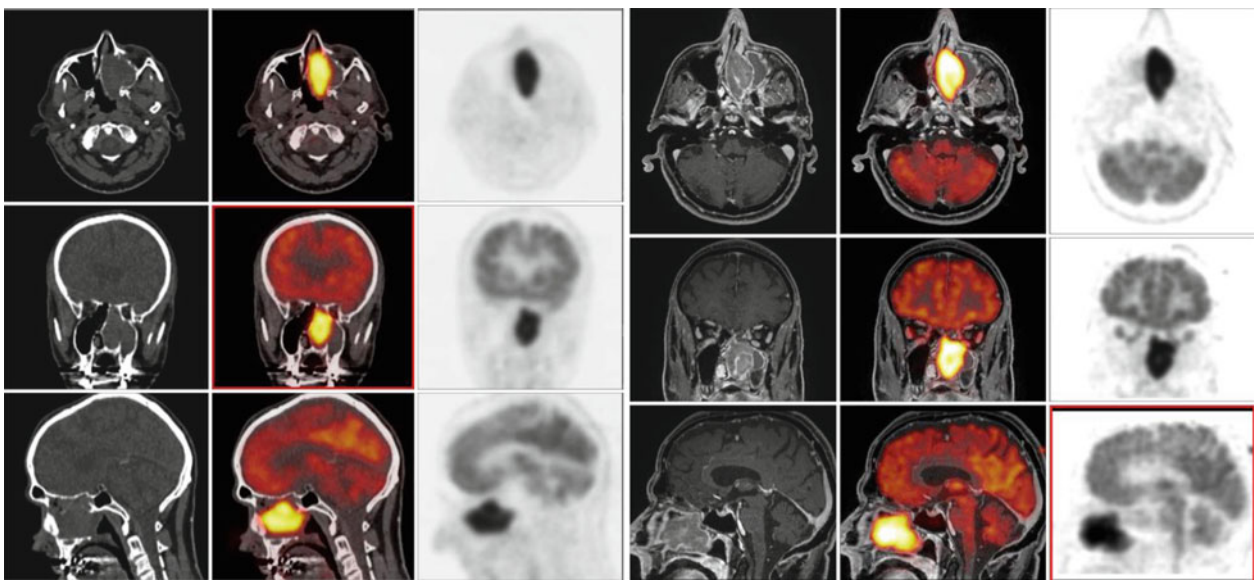

Fig. 4.11 Comparison of three orthogonal views centered around the nasal fossa lesion from PET/CT (*left*), and PET/MRI (*right*)

Retrocricoid Carcinoma

Clinical History

Sixty-two-year-old male with 62 pack years. Alcohol stopped since 1 year. The patient complained of dysphagia since 6 months, fatigue and weight loss of 8 kg. Initial PET/CT showed a retrocricoid tumor with a right-sided nodal metastasis. PET/CT and [18F]FDG-PET/MRI after radio-chemotherapy were performed for pre-operative evaluation.

Imaging Technique

Initial contrast-enhanced PET/CT. Unenhanced PET/CT and Gd-enhanced [18F]FDG-PET/MRI after chemo-radiotherapy. [18F]FDG-PET/MRI with axial T1w and T2w SE images, DWI images and 2D axial, coronal and sagittal 2D reformatted images of a high-resolution Dixon sequence obtained after intravenous administration of Gd.

Findings

PET/CT prior to chemoradiation shows a bulky bilateral retrocricoid tumor with a level III lymph node metastasis on the right. Both PET/CT and [18F]FDG-PET/MRI obtained after chemo-radiotherapy show only partial local response. The right level III lymph node metastasis, however, has disappeared.

Teaching Points

Retrocricoid tumors constitute between 2.5 and 3.5 % of all hypopharyngeal cancers. Tobacco and alcohol consumption are the main etiologic factors followed by the Plummer Vinson syndrome.

Retrocricoid HNSCC are often detected later than piriform sinus cancers because presenting symptoms are vague. Tumors are typically located submucosally and tend to spread downwards into the cervical esophagus. Lymph node metastases are seen in up to 75 % of cases at initial presentation. Cure is difficult to achieve.

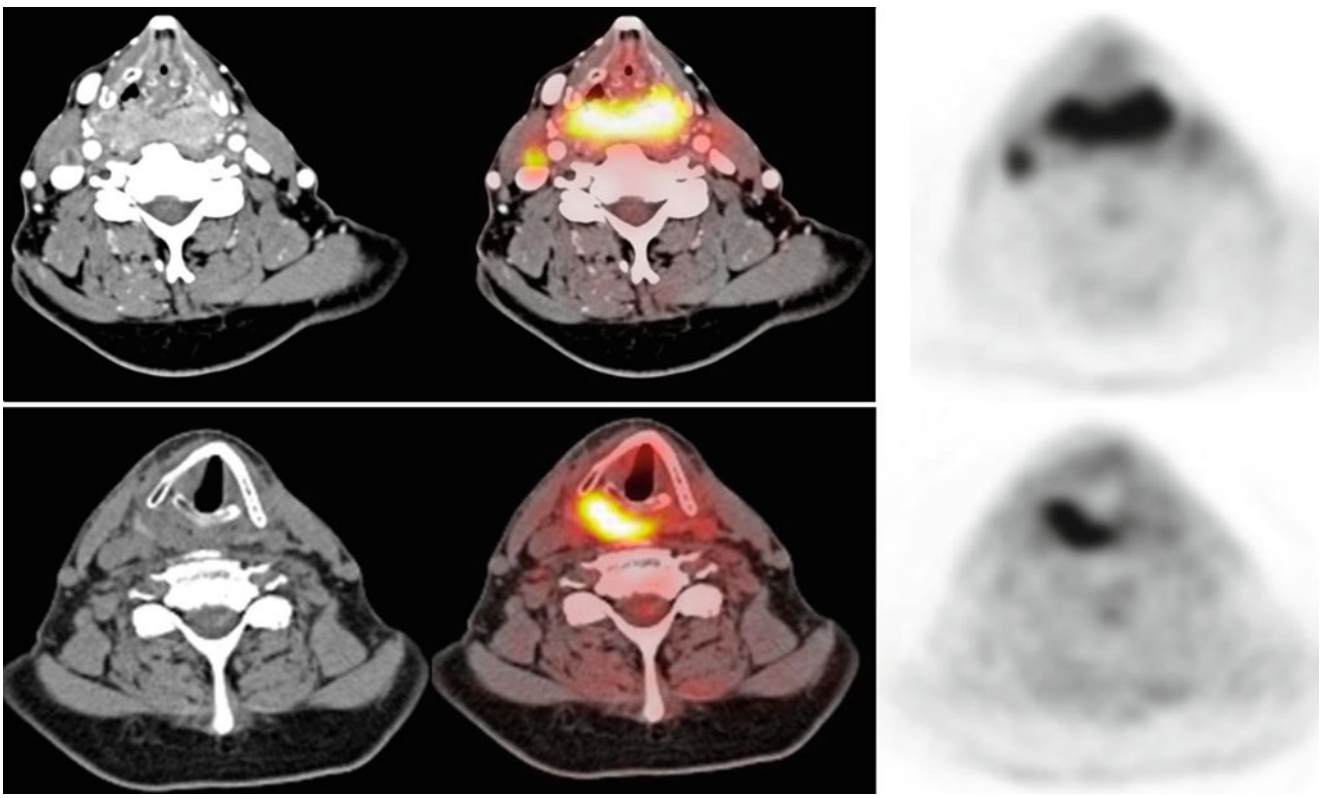

Fig. 4.12 PET/CT examinations before (*top*) and after chemoradiation (*bottom*) show major decrease of tumor volume and FDG uptake in the retrocricoid area and disappearance of the level III lymph node metastasis on the *right*

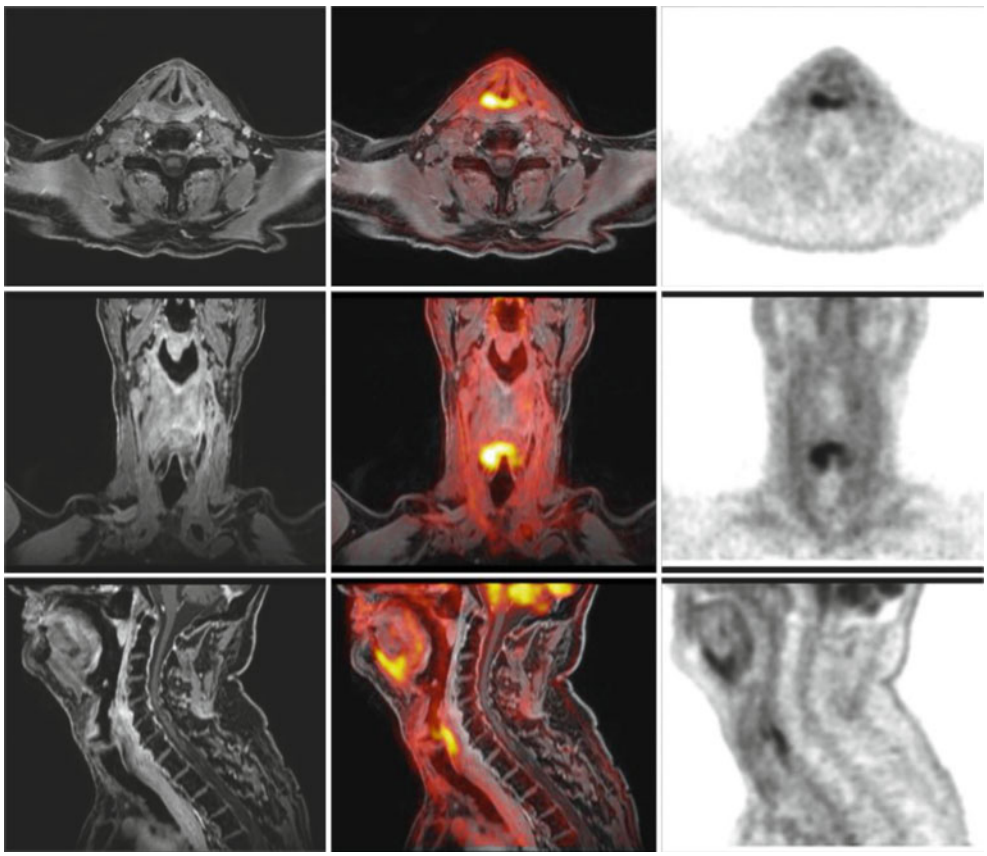

Fig. 4.13 Multi-planar reformatted PET/MRI images centered on the residual lesion allowing precise assessment of its cranio-caudal extent both on MRI and on fused PET/MRI images. The bilateral residual tumor spreads into the cervical esophagus. Note physiologic uptake of the sublingual glands on the sagittal reformatted images

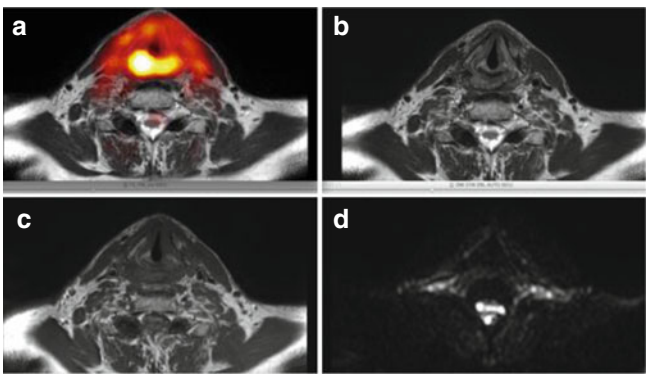

Fig. 4.14 Axial PET/MRI images at the level of the residual tumor: (**a**) Fused T2w TSE and PET (**b**) T2w TSE (**c**) T1w TSE (**d**) DWI. The tumor is easily seen on the first two images, however, it cannot be seen on the DWI image

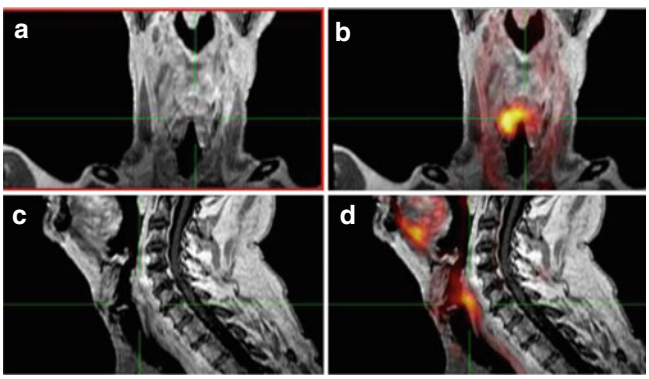

Fig. 4.15 Coronal and sagital PET/MRI images at the level of the residual tumor. Coronal T1w (**a**), sagittal T1w (**b**) and corresponding fused images (**c**, **d**). Same information as in Fig. 4.13. The T1w images are from the Dixon sequence

HNSCC of the Oropharynx with Lung Metastases

Clinical History

Fifty-five-year-old male with a history of radiotherapy for a T2N1M0 oropharyngeal HNSCC. Several years after initial treatment, the patient complained of odynophagia slowly increasing over a period of 1 year. Clinical examination revealed a base of the tongue tumor. Endoscopy revealed no other lesions.

Imaging Technique

Initial whole-body 18F-FDG PET/CT without contrast followed by Gd-enhanced PET/MRI that included whole body scan and axial T1w and T2w SE images, before and after intravenous administration of Gd.

Findings

PET/MRI shows a recurrent base of tongue tumor with a large area of ulceration best seen on the sagittal reconstructed images. There is involvement of a level VI lymph node on the right side, involvement of a pre-tracheal node and also multiple bilateral hypermetabolic nodules in the lungs suggesting metastatic lesions.

Teaching Points

PET is primarily used for the work-up of distant metastases and to look for synchronous tumors, which may be seen in up to 20 % of patients with HNSCC.

In recurrent tumors, the rate of synchronous second tumors and the probability of distant metastases is higher than in primary tumors.

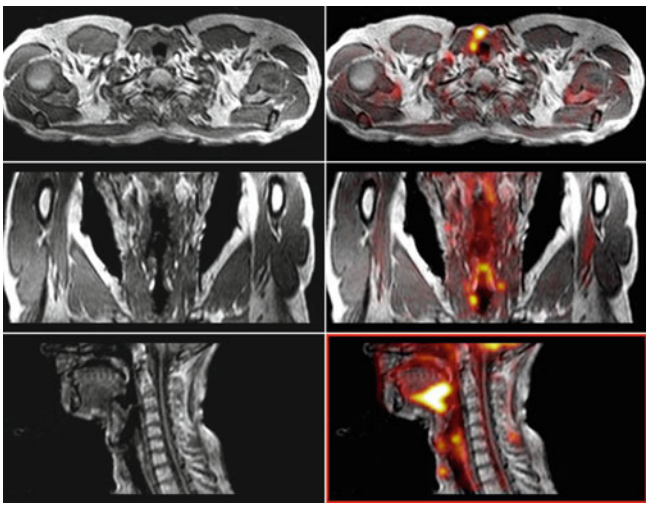

Fig. 4.16 2D multiplanar reformatted views of PET/MRI images of the base of the tongue tumor recurrence obtained from whole body low resolution T1W MRI used for localization of focal lesions on PET

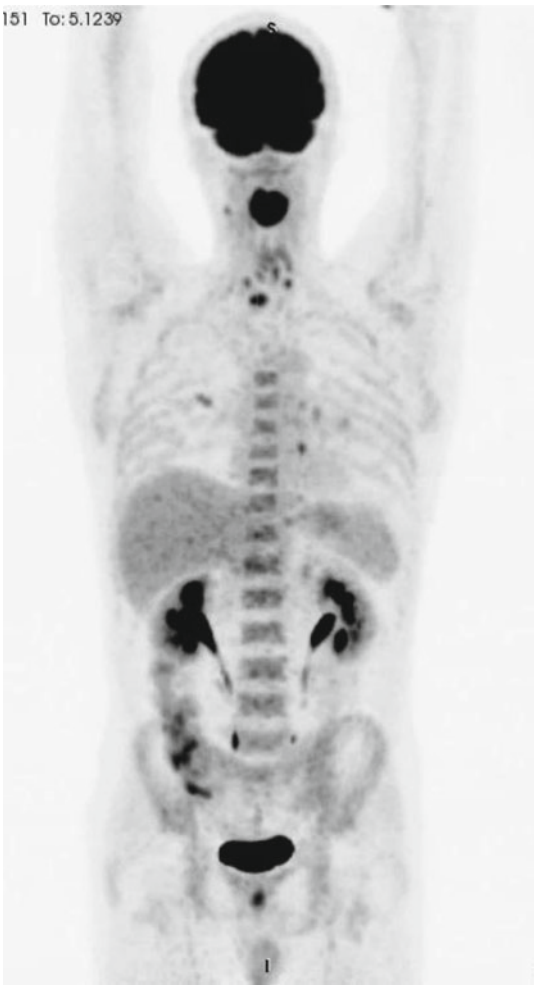

Fig. 4.17 Coronal MIP rendering of PET images showing the recurrent tumor and secondary focal lesions in the lungs

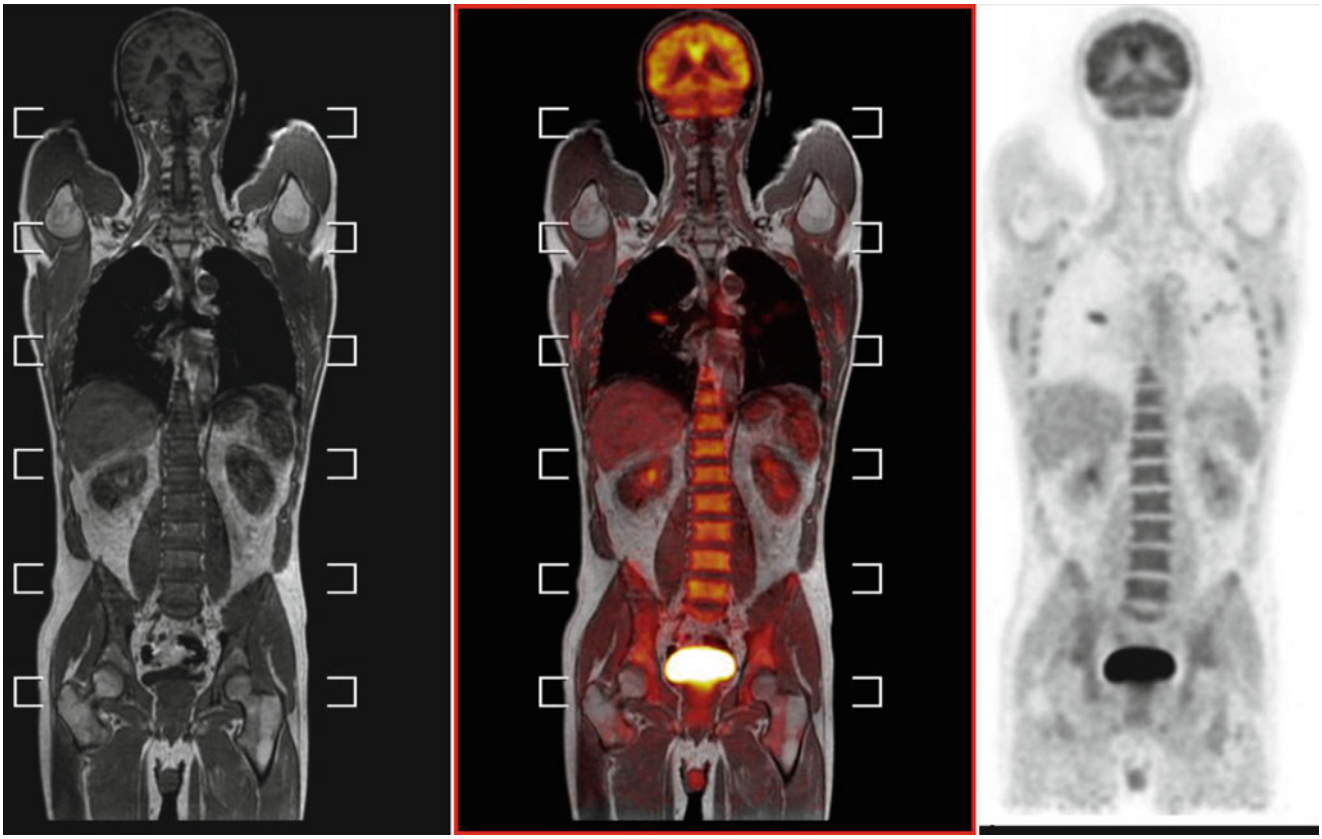

Fig. 4.18 Coronal views of whole body MRI (*left*), PET (*right*) and fusion of both (*middle*) showing lesions with focal FDG uptake in the lungs

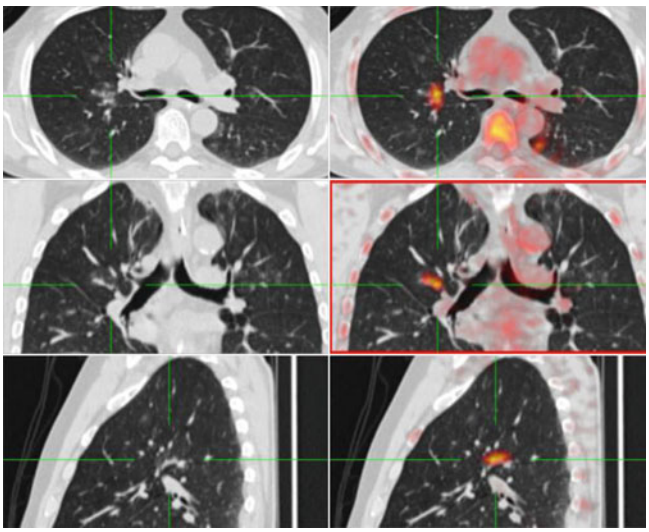

Fig. 4.19 Multiplanar reformatted PET/CT images in three orthogonal planes centered on the focal lesion of the right hilum

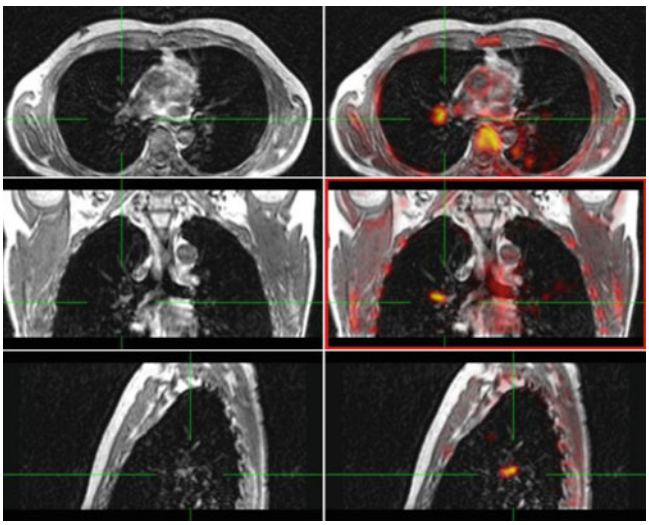

Fig. 4.20 Multiplanar reformatted PET/MRI images in three orthogonal planes centered on the focal lesion of the right hilum showing similar findings as on PET/CT. Biopsy confirmed lung metastases

SCCHN: Primary Staging

Clinical History

Forty-year-old HIV positive patient presenting with an ulcer at the floor the mouth on the left side and pain; biopsy revealed squamous cell carcinoma; patient is referred to PET/CT followed by PET/MR for primary staging.

Imaging Technique

Partial whole body PET/CT images acquired at 62 min after iv injection of 329 MBq 18F-FDG (7 bed positions a 2 min; with full diagnostic CT with i.v. contrast and dedicated head-and-neck study); PET/MR images acquired 92 min p.i., 52 kg.

Partial whole-body PET/MR: 4 beds × 4 min together with coronal T1w TSE and axial T2w haste fs. 1 bed (head-neck) a 15 min together with ax T1w ± Gd-DTPA, STIR ax and sag; T1w fatsat cor + Gd. Post CM axial T1w VIBE from chest to pelvis. Head/neck and TIM body coils.

Findings

The primary tumor on the left side of the floor of the mouth shows intense uptake of 18F-FDG and extends into the area of the left tonsil. The full extent and exact delineation of the tumor borders especially in the region of the left tonsil is better appreciated in the corresponding MR as compared to CT. Both CT and MR shows enlarged cervical lymph nodes on the left side. In PET, also smaller lymph nodes show intense tracer uptake, strongly suggesting lymph node metastases.

Teaching Points

For primary staging of squamous cell carcinoma of the head-and-neck area, MR is superior to CT for the delineation of primary tumors arising in the suprahyoid neck due to its excellent soft tissue contrast and can thus provide synergistic information together with 18F-FDG PET.

Concerning assessment of lymph nodes, PET can provide additional information in non-enlarged lymph nodes, suggesting malignancy despite of small size when the uptake is intense. On the other hand, the morphologic information of MR (or CT) is mandatory, because necrotic malignant lymph nodes can show only weak or moderate uptake, but can usually be defined as clearly malignant based on morphological criteria. This shows the synergistic value of morphological and biological imaging.

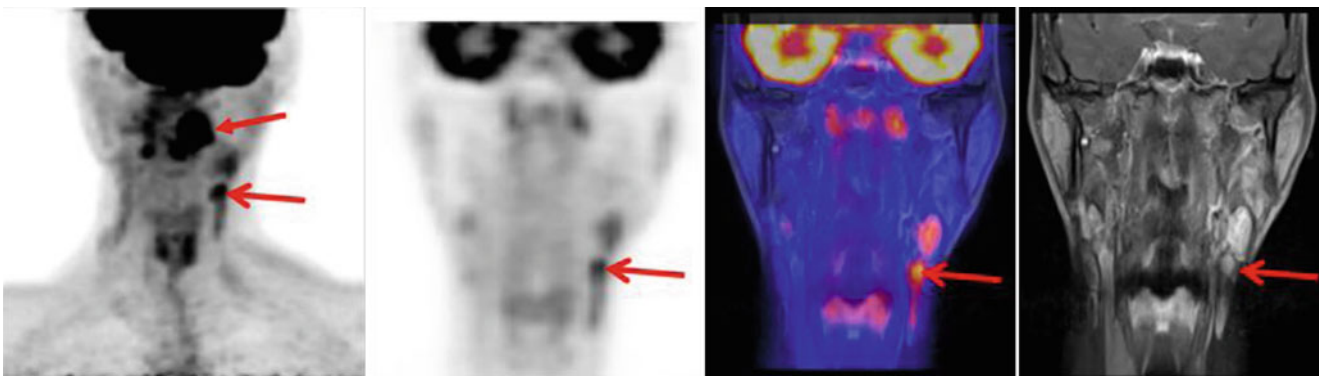

Fig. 4.21 PET/MR images from the head-and-neck area (*from left* to *right*): in the MIP of the PET you see the intense uptake in the primary tumor (*arrow*, *closed tip*) and several lymph nodes with variable uptake on the *left side*, the most intense one is marked with an *arrow* (*open tip*). The larger one directly above shows lesser uptake, but shows morphological criteria for malignancy, the small one marked with the *arrow* is unremarkable morphologically, however due to its intense uptake also has to be considered suspicious for malignancy

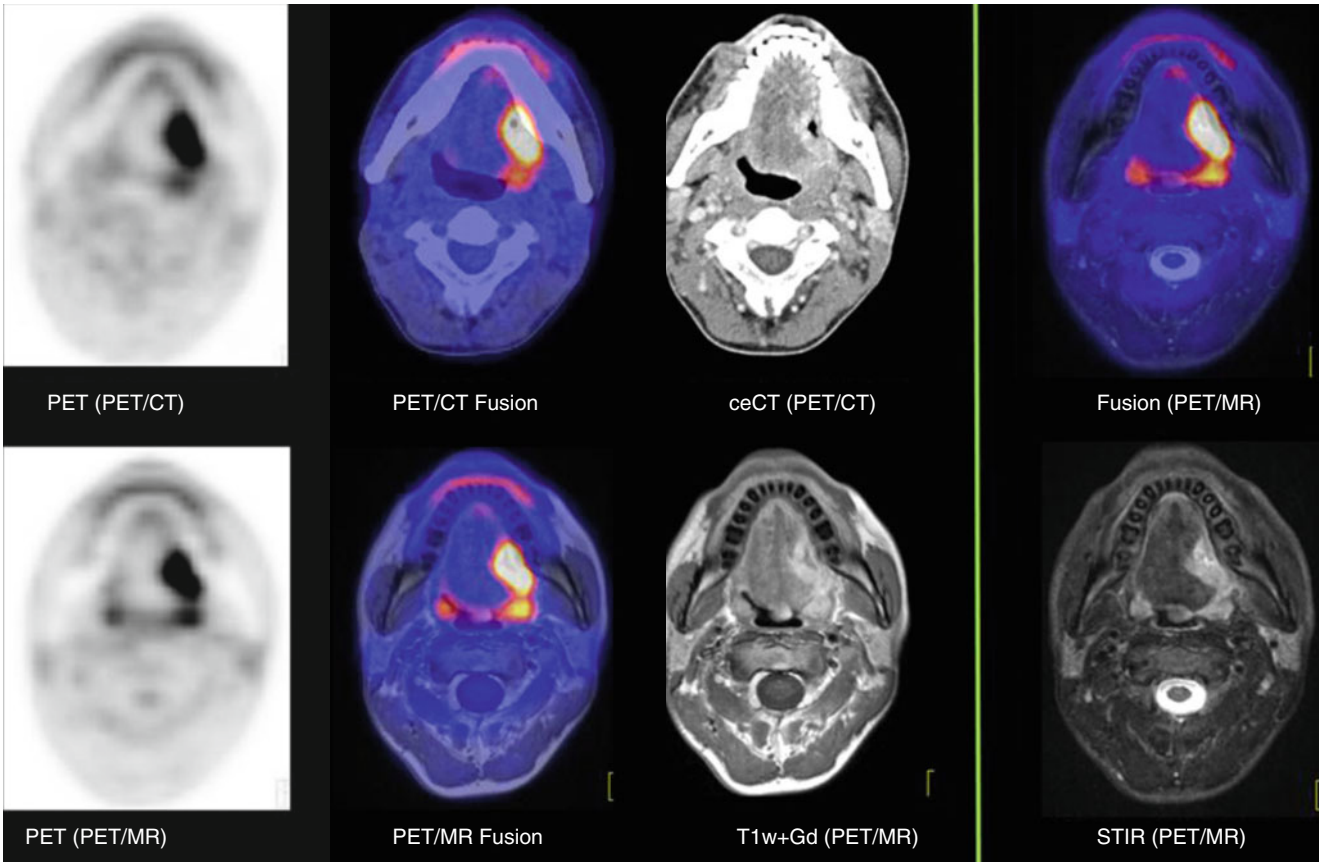

Fig. 4.22 Comparison PET/CT and PET/MR concerning the primary tumor (first 3 images *upper row* PET/CT, *lower row* PET/MR): the primary tumor shows intense 18F-FDG uptake, which can be clearly seen on both PET/CT and PET/MR. However the tumor borders and the extension of the tumor towards the left tonsillar area are better defined in the corresponding MR images as compared to CT. Note absence of mandibular invasion

SCCHN: Primary Staging, Dental Implants Artifacts

Clinical History

Fifty-three-year-old patient presenting with an ulcer at the right side of the tongue; biopsy revealed squamous cell carcinoma; patient is referred to PET/CT followed by PET/MR for primary staging.

Imaging Technique

Upper body PET/CT images acquired at 60 min after iv injection of 362 MBq 18F-FDG (6 bed positions a 2 min; with full diagnostic CT with i.v. contrast and dedicated head-and-neck study); PET/MR images acquired 94 min p.i., 64 kg.

Head and thoracic PET/MR: 4 beds × 4 min together with coronal T1w TSE and axial T2w haste fs. 1 bed (head-neck) a 15 min together with ax T1w ± Gd-DTPA, STIR ax and sag; T1w fatsat cor + Gd. Post CM axial T1w VIBE from chest to pelvis. Head/neck and TIM body coils.

Findings

The primary tumor involving the right anterior mobile tongue shows intense focal uptake of 18F-FDG both on PET from PET/CT and PET/MR. However due to extensive artefacts from dental implants adjacent to the tumor, the full extent and exact delineation of the tumor borders cannot be evaluated in the CT. However, in the MR from PET/MR, the exact tumor borders can be nicely seen, in particular involvement of the midline, undersurface of the right tongue and sublingual space. The tumor reaches the midline without crossing it. Both CT and MR show enlarged heterogeneous cervical lymph nodes on the right side in level 2, probably partially necrotic. In PET, weak to moderate tracer uptake is seen.

Teaching Points

In primary staging of SCCHN, delineation of the primary tumor in CT is often impaired by artefacts from adjacent dental implants. Depending on the imaging sequence, this can be less pronounced in MR.

However for lymph node staging, diagnostic CT with multiplanar reformations is at least equally good as MRI, especially in patients with low compliance due to the rather long examination times necessary for a comprehensive MR examination.

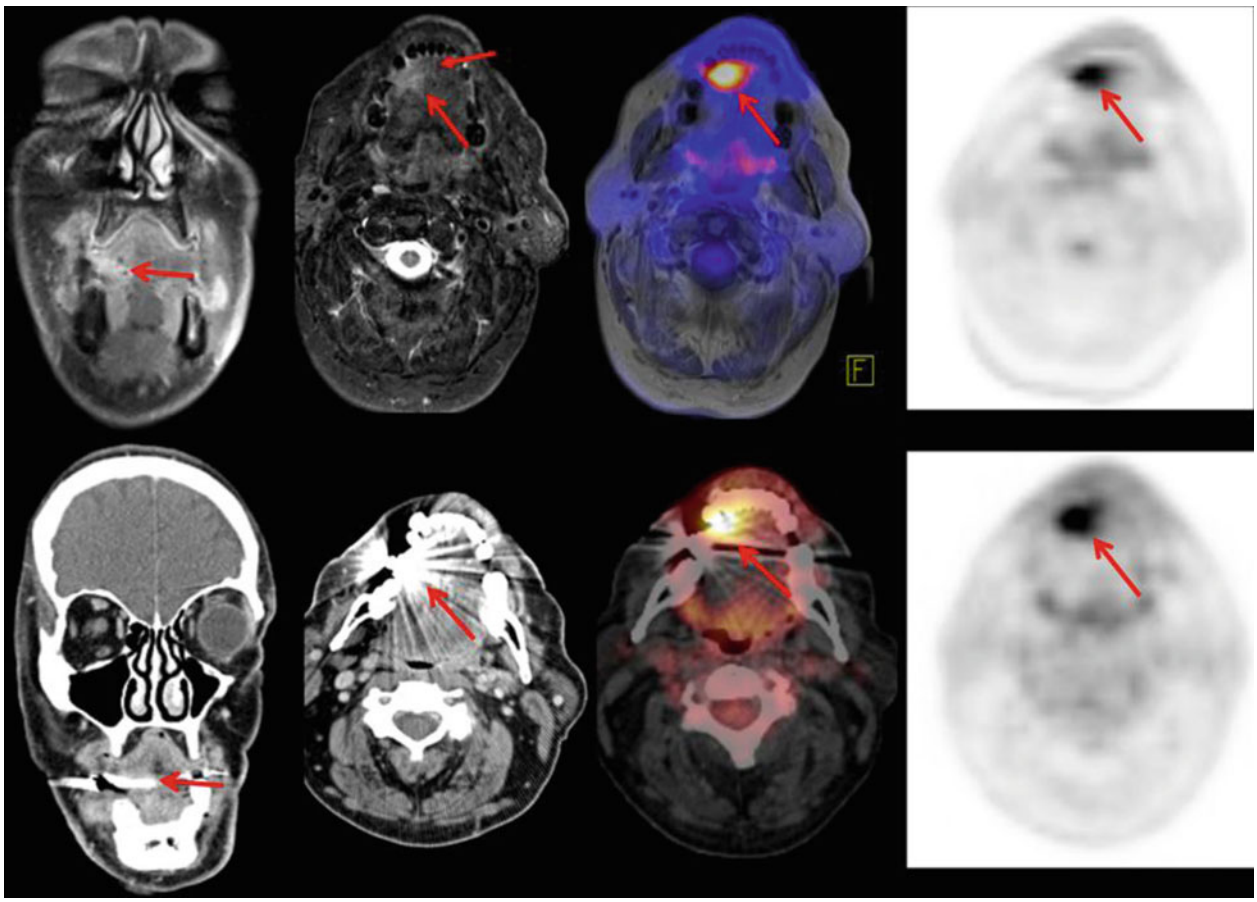

Fig. 4.23 PET/MR images (*upper row*) and PET/CT (*lower row*) from the head-and-neck area: the primary tumor (*arrow*, *open tip*) shows intense tracer uptake, but cannot be delineated on CT due to artefacts from adjacent dental implants. However in the MR from PET/MR, the tumor can be seen very well. The tumor borders reach but do not cross the midline (*arrow*, *closed tip*)

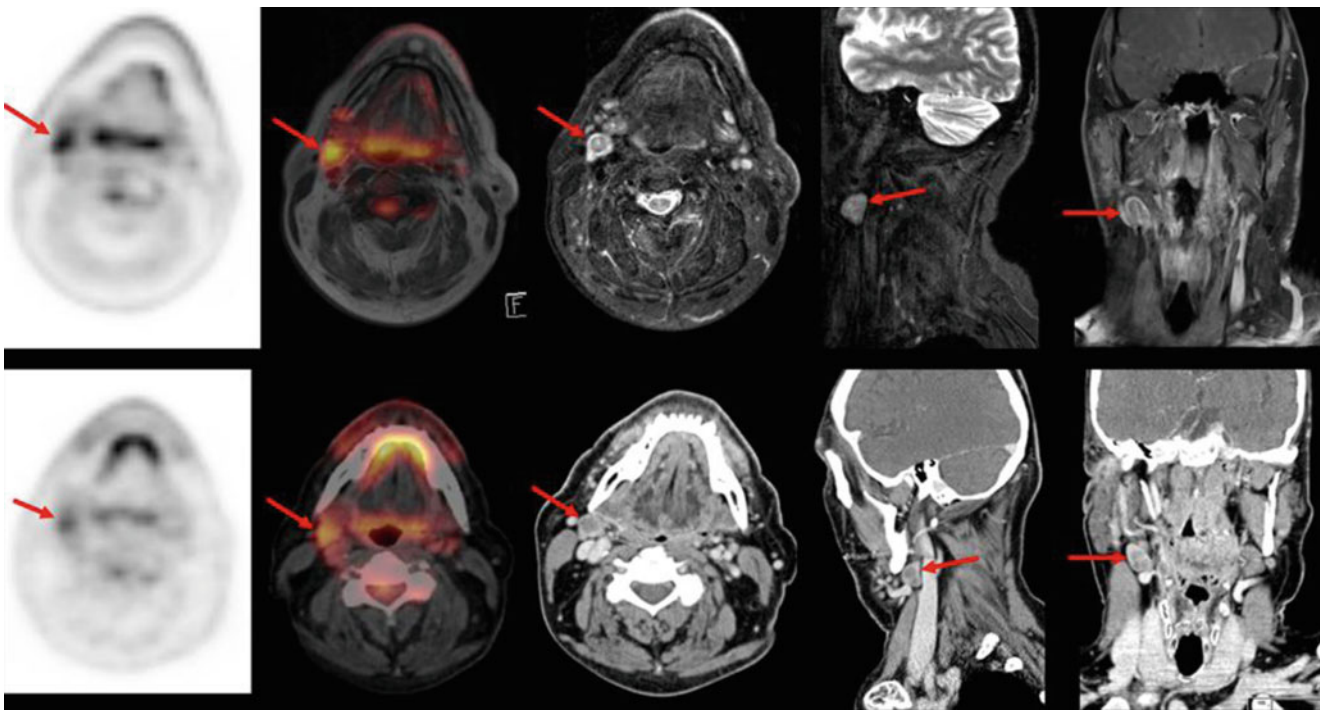

Fig. 4.24 Comparison of PET/CT and PET/MR concerning lymph node staging (*upper row* PET/MR, *lower row* PET/CT): the lymph node on the *right side* level 2 shows weak to moderate 18F-FDG uptake (*arrows*). However, both CT and MRI show substantial heterogeneity of the lymph node with a high signal on T2w images and peripheral rim enhancement on CT and MRI characteristic of central nodal necrosis. Thus the lymph node clearly has to be called metastatic. This also explains why the 18F-FDG uptake is not more intense. Here both PET/MR and PET/CT with diagnostic CT and multiplanar reformation perform equally well for lymph node assessment

SCCHN: Multiparametric Imaging

Clinical History

Seventy-six-year-old patient presenting with a bioptically proven squamous cell carcinoma of the left tonsil; patient is referred to PET/CT followed by PET/MR for primary staging and planning of radiochemotherapy.

Imaging Technique

Upper body PET/MR images acquired at 89 min after iv injection of 440 MBq 18F-FDG, 96 kg. 4 beds×4 min together with coronal T1w TSE and axial T2w haste fs. 1 bed (head-neck) a 15 min together with STIR ax and cor; DWI ax (b 50, 400, 800); Head/neck and TIM body coils.

Findings

The primary tumor in the left tonsil shows intense focal uptake of 18F-FDG in PET/MR. There are no enlarged or morphologically suspicious lymph nodes visible. However, in PET a moderate tracer uptake is seen in one small lymph node on the left side level 2. In the DWI images and the corresponding ADC map, we can see substantial restricted water movement in the primary tumor, which is better delineated from the surrounding tissue as compared to the STIR images alone. The area with low ADC values corresponds well to the area with intense 18F-FDG uptake. Note a small lymph node with the moderate tracer uptake shows low ADC values that is clearly delineated in the DWI images. The combination of low ADC values and tracer uptake suggest malignancy despite the small size.

Teaching Points

Combining functional information from MRI, like DWI or also DCE-MRI and MRS with the biological information from PET is feasible with high spatial precision with combined PET/MR.

In SCCHN, this combined information of DWI and biological information from PET might provide synergistic information on tumor biology, which in the future might be helpful for radiation therapy planning and/or classification of lymph nodes.

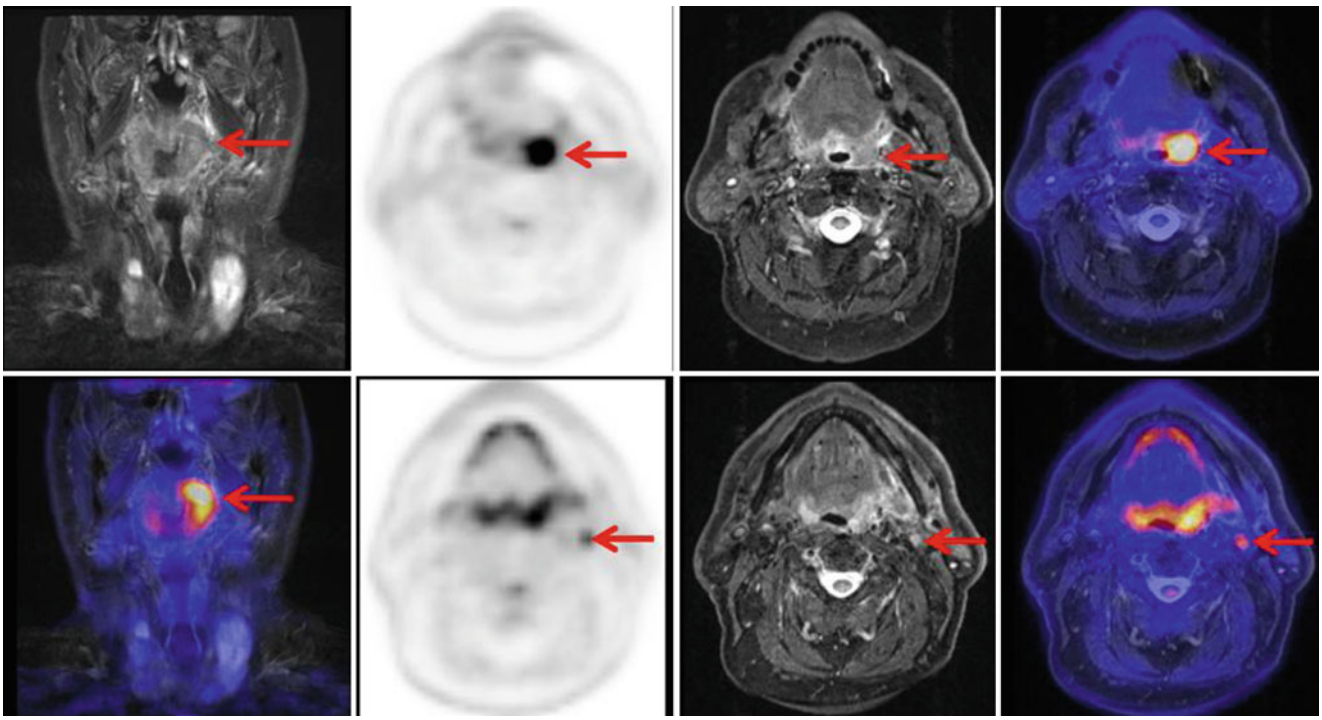

Fig. 4.25 PET/MR images from the head-and-neck area show the primary tumor (*upper row*, *arrows*) and lymph node on the *left side* level 2 (*lower row*, *arrows*): the primary tumor shows intense tracer uptake. The lymph node is small and shows only moderate tracer uptake, meaning that it could either be malignant or an unspecific benign reactive lymph node

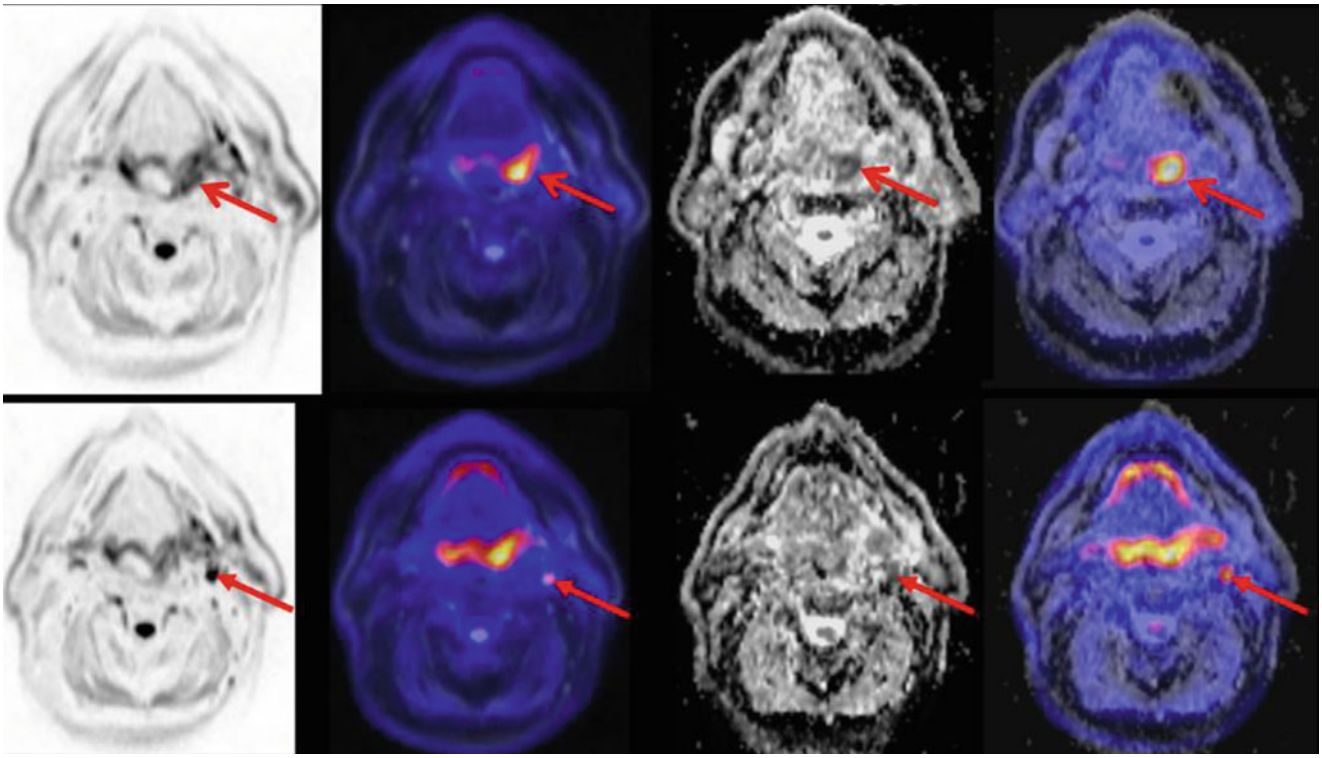

Fig. 4.26 Comparison of DWI and 18F-FDG PET in PET/MR for multiparametric imaging of tumor biology: primary tumor in the *upper row* (*arrow*, *open tips*), lymph node in the *lower row* (*arrow*, *closed tip*); *from left* to *right*: in the b 400 DWI images, the primary tumor and especially the small lymph node can be delineated very well, corresponding to the areas of tracer uptake in the DWI-PET fused images. On ADC maps we can also see the areas of restricted water movement with low ADC values corresponding to the areas of tracer uptake in the PET/ADC map fused images

Further Reading

Buchbender C, Heusner TA, Lauenstein TC, Bockisch A, Antoch G (2012) Oncologic PET/MRI, part 1: tumors of the brain, head and neck, chest, abdomen, and pelvis. J Nucl Med 53(6):928–938

Eiber M, Souvatzoglou M, Pickhard A et al (2012) Simulation of a MR-PET protocol for staging of head-and-neck cancer including Dixon MR for attenuation correction. Eur J Radiol 81(10): 2658–2665

Loeffelbein DJ, Souvatzoglou M, Wankerl V et al (2012) PET/MRI fusion in head-and-neck oncology: current status and implications for hybrid PET/MRI. J Oral Maxillofac Surg 70(2): 473–483

Nakamoto Y, Tamai K, Saga T et al (2009) Clinical value of image fusion from MR and PET in patients with head and neck cancer. Mol Imaging Biol 11(1):46–53

Platzek I, Beuthien-Baumann B, Schneider M et al (2013) PET/MRI in head and neck cancer: initial experience. Eur J Nucl Med Mol Imaging 40(1):6–11

Vargas MI, Becker M, Garibotto V et al (2013) Approaches for the optimization of MR protocols in clinical hybrid PET/MRI studies. MAGMA 26(1):57–69